

# Synthesis, Structure and Reactivity of Bis(phosphido)-Bridged Dinuclear Carbonyls of Platinum(I)

Alberto Albinati,<sup>[a]</sup> Piero Leoni,<sup>\*[b]</sup> Fabio Marchetti,<sup>[b]</sup> Lorella Marchetti,<sup>[b]</sup> Marco Pasquali,<sup>[b]</sup> and Silvia Rizzato<sup>[a]</sup>

**Keywords:** Platinum / Dinuclear complexes / Bridging ligands / Crystal structures / Phosphanes / Phosphido ligands

The platinum(I) dinuclear carbonyl  $[\text{Pt}_2(\mu\text{-PtBu}_2)_2(\text{PtBu}_2\text{H})(\text{CO})]$  (**4**) reacts with carbon monoxide (80 atm) to give the dicarbonyl complex  $[\text{Pt}(\mu\text{-PtBu}_2)(\text{CO})]_2$  (**9**), which is thermally and air stable if protected from moisture. Wet solvents convert **9** into the known trinuclear hydride  $\text{Pt}_3(\mu\text{-PtBu}_2)_3(\text{CO})_2\text{(H)}$  (**10**), which is also formed by treating **9** with molecular hydrogen (180 atm). The reaction of **4** or **9** with phosphanes  $[\text{PR}_3 = \text{PMe}_3, \text{PPh}_3, \text{PCy}_3, \text{PCy}_2\text{H}]$  results in the formation of the corresponding derivatives  $[\text{Pt}_2(\mu\text{-PtBu}_2)_2(\text{PtBu}_2\text{H})(\text{PR}_3)]$  [**11**, R = Me; **12**, R = Ph; **13**, R = Cy; **14**, R<sub>3</sub> = Cy<sub>2</sub>H],  $[\text{Pt}_2(\mu\text{-PtBu}_2)_2(\text{CO})(\text{PR}_3)]$  [**15**, R = Me; **16**, R = Ph; **17**, R = Cy] or  $[\text{Pt}(\mu\text{-PtBu}_2)(\text{PR}_3)]_2$  [**18**, R = Me; **19**, R = Ph; **20**, R = Cy] in good yields. Complex **19** is protonated at platinum by  $\text{CF}_3\text{SO}_3\text{H}$  yielding the hydride  $[\text{Pt}_2(\mu\text{-PtBu}_2)_2(\text{H})(\text{PPh}_3)_2]\text{-}$

$\text{CF}_3\text{SO}_3$  (**21**). The protonation of asymmetrically substituted **12** forms rapidly the kinetic hydride  $[(t\text{Bu}_2\text{HP})\text{Pt}(\mu\text{-PtBu}_2)_2\text{-Pt(H)(PPh}_3)]\text{CF}_3\text{SO}_3$  (**22a**), which then isomerises slowly to the more stable isomer  $[(\text{Ph}_3\text{P})\text{Pt}(\mu\text{-PtBu}_2)_2\text{Pt(H)(PtBu}_2\text{H})]\text{-CF}_3\text{SO}_3$  (**22b**). Dicarbonyl **9** is instead protonated at the phosphorus atom of a bridging phosphide; the unstable product of this reaction can be intercepted by adding CO to give the monophosphido-bridged  $[\text{Pt}_2(\mu\text{-PtBu}_2)(\text{PtBu}_2\text{H})(\text{CO})_3]\text{CF}_3\text{SO}_3$  (**24**) as a mixture of two isomers. The X-ray crystal and molecular structures of **9**, of a 2:1 mixture of **9** and **10**, and of complexes **18**, **19** and **21** are also reported.

(© Wiley-VCH Verlag GmbH & Co. KGaA, 69451 Weinheim, Germany, 2008)

## Introduction

Terminal phosphides are generally protonated at the phosphorus atom.<sup>[1a–1g]</sup> By contrast, with a few exceptions,<sup>[1h]</sup> one metal centre (or the metal–metal bond) is the stronger basic site in bridging metal phosphides.<sup>[1h,2]</sup> In our previous papers we showed that the palladium bis(phosphido)-bridged dinuclear derivative  $\text{Pd}_2(\mu\text{-PtBu}_2)_2\text{(PtBu}_2\text{H)}_2$  (**1**)<sup>[3a]</sup> (Scheme 1) is protonated at one bridging phosphorus to afford the Pd–H–P agostic palladium(I) derivative  $[\text{Pd}_2(\mu\text{-PtBu}_2)(\mu\text{-PtBu}_2\text{H})(\text{PtBu}_2\text{H})_2]\text{CF}_3\text{SO}_3$  (**2**).<sup>[3b,3c]</sup> We also reported that the bridging secondary phosphane may be easily displaced from **2**, thus significantly reducing the steric hindrance around the metal–metal bond and allowing the formation of monophosphido-bridged systems where the Pd centres cooperate in the coordination of new ligands.<sup>[3d–3f]</sup> The platinum analogue of **1**, and its monocarbonyl derivative, **3**<sup>[4a]</sup> and **4**<sup>[4b]</sup> in Scheme 1,

are instead protonated at one metal centre, to afford the Pt<sup>II</sup> hydrides  $[\text{Pt}_2(\mu\text{-PtBu}_2)_2(\text{H})(\text{L})(\text{L}')]\text{CF}_3\text{SO}_3$  (**5–6a,b**).<sup>[4a,4c]</sup>

As theoretically predicted,<sup>[4c]</sup> in the presence of new ligands the platinum-bonded hydride of these derivatives may be transferred to the adjacent bridging phosphorus.<sup>[4d]</sup> When this occurs (cation **6b**<sup>+</sup>), the overall reactivity of the dinuclear palladium or platinum cations is similar, despite the different site of proton attack. In some cases, however (cations **5**<sup>+</sup> and **6a**<sup>+</sup>), the platinum cations fail to give the hydride-transfer reaction, and therefore, is much less reactive.<sup>[4d]</sup>

Moreover, we recently found that the protonation of the bis(ethylene) derivative  $\text{Pt}_2(\mu\text{-PtBu}_2)_2(\eta^2\text{-CH}_2=\text{CH}_2)_2$ , (**7**) affords the secondary phosphane-bridged cation  $[\text{Pt}_2(\mu\text{-PtBu}_2)(\mu\text{-PtBu}_2\text{H})(\eta^2\text{-CH}_2=\text{CH}_2)_2]^+$  (**8**).<sup>[4e]</sup>

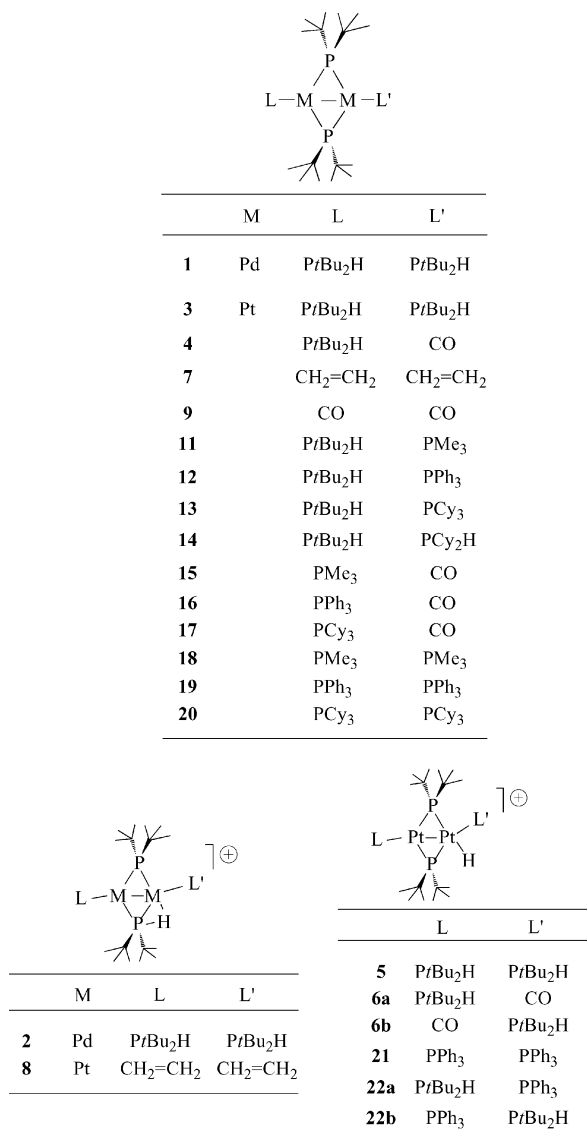
With the aim to investigate how ligands L, L' influence the site of protonation of the bis(phosphido)-bridged platinum derivatives and the reactivity of the resulting cations, we prepared a series of new  $[\text{Pt}_2(\mu\text{-PtBu}_2)_2(\text{L})(\text{L}')]$  complexes. The results of this study are discussed herein.

## Results and Discussion

An orange toluene solution of complex **4**<sup>[4b]</sup> was pressurised (80 atm) in an autoclave under a CO atmosphere. After stirring for 12 h at 25 °C and workup,  $[\text{Pt}(\mu\text{-PtBu}_2)(\text{CO})]_2$

[a] Dipartimento di Chimica Strutturale e Facoltà di Farmacia, Università di Milano, Via Venezian 21, I-20133 Milano, Italy. Fax: +39-02-50314454. E-mail: alberto.albinati@unimi.it

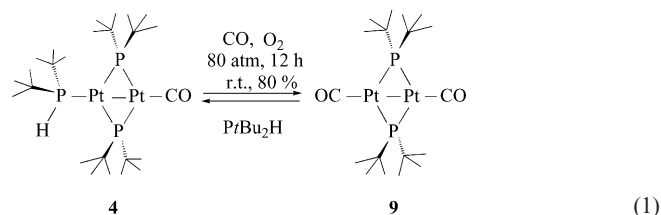
[b] Dipartimento di Chimica e Chimica Industriale, Università di Pisa, Via Risorgimento 35, 56126 Pisa, Italy. Fax: +39-050-2219240. E-mail: leoni@dccl.unipi.it



Scheme 1.

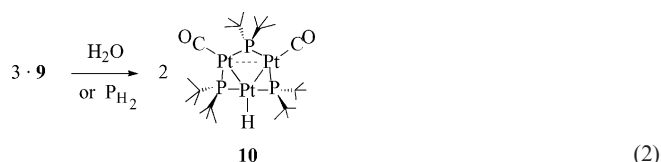
(**9**) was isolated as an orange microcrystalline solid. Complex **9** is thermally stable and is not oxidised by dry oxygen, either in the solid state or in solution, but it is easily converted by moisture into the known<sup>[5]</sup> trinuclear hydride Pt<sub>3</sub>(μ-*Pr*Bu<sub>2</sub>)<sub>3</sub>(CO)<sub>2</sub>(H) (**10**; see below). Therefore, **9** can be obtained in good yields only under strictly anhydrous conditions; moreover, the addition of a molar excess of dry oxygen is essential to drive the equilibrium [Equation (1)] towards the formation of complex **9**, by oxidising the secondary phosphane to O=*Pr*Bu<sub>2</sub>H.

Under the better conditions, **4** was nearly quantitatively (<sup>31</sup>P{<sup>1</sup>H} NMR) converted into **9**, which was then isolated in 80% yield. Complex **9** was also obtained by treating **4** with 1 atm of O<sub>2</sub>/CO (1:10) for 12 h at 60 °C, although in a mixture with small (<10%) amounts of unidentified impurities. The structure shown in Equation (1) can easily be assigned to complex **9** on the basis of its spectroscopic features, and it was confirmed by a crystallographic study (see below).



The <sup>31</sup>P{<sup>1</sup>H} NMR spectrum (C<sub>6</sub>D<sub>6</sub>, 293 K) exhibits a singlet with <sup>195</sup>Pt satellites [comprising a 1:8:18:8:1 quintet with  $J = {}^1J(\text{P,Pt})/2$ ]<sup>[6]</sup> at low fields [ $\delta = 305.4$  ppm,  ${}^1J(\text{P,Pt}) = 2493$  Hz], and the <sup>195</sup>Pt{<sup>1</sup>H} NMR spectrum gives a triplet at  $\delta = -5235$  ppm [ ${}^1J(\text{P,Pt})$  see above], as expected for two equivalent P nuclei bridging two equivalent (metal-metal bonded)<sup>[7]</sup> platinum centres. <sup>1</sup>H and <sup>13</sup>C{<sup>1</sup>H} NMR spectra (see the Experimental Section) are consistent with structure **9**. A single  $\nu_{\text{CO}}$  absorption was found at 1980 cm<sup>-1</sup> in the IR spectrum, and the increase in the  $\nu_{\text{CO}}$  relative to **4** (1956 cm<sup>-1</sup>) is due to the substitution of a basic phosphane with the  $\pi$ -acceptor CO ligand.

Complex **10**, which is formed under wet conditions together with other unidentified byproducts, was unequivocally identified by its <sup>1</sup>H, <sup>31</sup>P{<sup>1</sup>H} and <sup>195</sup>Pt{<sup>1</sup>H} NMR spectra,<sup>[5]</sup> and it was also formed in higher yields (>65%) when a toluene solution of **9** was pressurised under H<sub>2</sub> (180 atm) under strictly anhydrous conditions [Equation (2)]. The carbonyl ligand(s) contained in complexes **4** and **9** can be easily substituted by tertiary phosphanes [PR<sub>3</sub> = PMe<sub>3</sub>, PPh<sub>3</sub>, PCy<sub>3</sub>], thus providing easy access to the unsymmetrically substituted [Pt<sub>2</sub>(μ-*Pr*Bu<sub>2</sub>)<sub>2</sub>(*Pr*Bu<sub>2</sub>H)(PR<sub>3</sub>)] [**11**, R = Me; **12**, R = Ph; **13**, R = Cy; **14**, R<sub>3</sub> = Cy<sub>2</sub>H] and [Pt<sub>2</sub>(μ-*Pr*Bu<sub>2</sub>)<sub>2</sub>(CO)(PR<sub>3</sub>)] [**15**, R = Me; **16**, R = Ph; **17**, R = Cy] or to the symmetrical derivatives [Pt(μ-*Pr*Bu<sub>2</sub>)-(PR<sub>3</sub>)<sub>2</sub>] [**18**, R = Me; **19**, R = Ph; **20**, R = Cy] (Scheme 1).

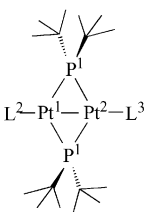


The structures of complexes **11**–**20**, isolated in good yields and purity, were straightforwardly assigned on the basis of their spectroscopic features (see IR and NMR parameters in Table 1 and in the Experimental Section).

Single crystals of complexes **18** and **19** were obtained by recrystallisation from CH<sub>2</sub>Cl<sub>2</sub>/DME or from toluene. Crystals of **9** were obtained by recrystallisation from acetone. During one of the recrystallisation attempts, an acetonitrile solution of **9** came accidentally in contact with air and single crystals containing a 2:1 mixture of **9** and **10** were obtained. There are no unusual packing interactions between the molecules of the two complexes, and their molecular geometries are comparable (within 3σ) to those observed in the crystals of pure **9** (see below) and **10**.<sup>[5]</sup> ORTEP plots of the structures of **9**, **18** and **19** are shown in Figures 1, 2

Table 1. Selected NMR parameters for complexes **4–13**.

	L <sup>2</sup>	L <sup>3</sup>	
	PrBu <sub>2</sub> H	PMe <sub>3</sub>	<b>11</b>
	PrBu <sub>2</sub> H	PPh <sub>3</sub>	<b>12</b>
	PrBu <sub>2</sub> H	PCy <sub>3</sub>	<b>13</b>
	PrBu <sub>2</sub> H	PCy <sub>2</sub> H	<b>14</b>
	CO	PMe <sub>3</sub>	<b>15</b>
	CO	PPh <sub>3</sub>	<b>16</b>
	CO	PCy <sub>3</sub>	<b>17</b>
	PMe <sub>3</sub>	PMe <sub>3</sub>	<b>18</b>
	PPh <sub>3</sub>	PPh <sub>3</sub>	<b>19</b>
	PCy <sub>3</sub>	PCy <sub>3</sub>	<b>20</b>

	<b>11</b>	<b>12</b>	<b>13</b>	<b>14</b>	<b>15</b>	<b>16</b>	<b>17</b>	<b>18</b>	<b>19</b>	<b>20</b>
$\delta(\text{P}^1)$	283.7, dd	276.4, dd	272.8, dd	285.2, dd	302.3, d	289.3, d	292.6, d	289.1, t	269.5, t	271.8, t
$\delta(\text{P}^2)$	61.8, dt	64.0, dt	62.2, dt	66.0, dt	—	—	—	−25.7, t	40.2, t	42.1, t
$\delta(\text{P}^3)$	−25.2, dt	42.4, dt	49.2, dt	20.3, dt	−18.3, t	44.2, t	56.5, t	−25.7, t	40.2, t	42.1, t
$\delta(\text{Pt}^1)$	−5432, dt	−5534, dt	−5572, dt	−5543, dt	−5297, dt	−5394, dt	−5415, dt	−5421, dt	−5459, dt	−5550, dt
$\delta(\text{Pt}^2)$	−5587, dt	−5527, dt	−5523, dt	−5592, dt	−5168, t	−5156, t	−5143, t	−5421, dt	−5459, dt	−5550, dt
$^1J(\text{P}^1, \text{Pt}^1)$	2515	2565	2618	2560	2552	2615	2666	2560	2567	2603
$^1J(\text{P}^1, \text{Pt}^2)$	2624	2578	2609	2590	2438	2416	2378	2560	2567	2603
$^1J(\text{P}^2, \text{Pt}^1)$	4759	4696	4743	4773	—	—	—	4802	5055	4797
$^1J(\text{P}^3, \text{Pt}^2)$	4792	5050	4795	4714	4686	4950	4698	4802	5055	4797
$^2J(\text{P}^1, \text{P}^2)$	53.6	41.1	42.8	43.2	—	—	—	52.6	47.0	46.6
$^2J(\text{P}^1, \text{P}^3)$	42.8	48.7	44.8	45.4	47.0	42.7	39.5	52.6	47.0	46.6
$^3J(\text{P}^2, \text{P}^3)$	73.3	75.8	73.2	71.8	—	—	—	—	—	—

and **3**, whereas significant bond lengths and angles are given in Table 2. The structures are similar to those of the few related derivatives  $[\text{M}_2(\mu\text{-PR}_2)_2(\text{L})(\text{L}')] (M = \text{Ni},^{[8]}\text{Pd},^{[3a,9]}\text{Pt}^{[4b,4e,10]})$  structurally characterised, with a planar, metal–metal bonded  $\text{Pt}_2(\mu\text{-P})_2\text{E}_2$  ( $E = \text{C}$  or  $\text{P}$ ) core.

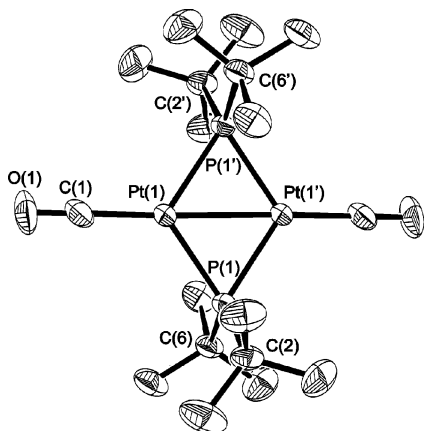


Figure 1. Perspective view of the molecular structure of **9**. Thermal ellipsoids are at 30% probability. Primed atoms are obtained by the symmetry operation:  $1 - x, -y, 1 - z$ .

Neglecting the Pt–Pt bond, each metal exhibits a trigonal planar coordination. The Pt–Pt distances at 2.5999(8), 2.6053(4) and 2.6126(2) Å for **9**, **18** and **19**, respectively, are comparable to those observed in **4** [2.6127(6) Å],<sup>[4b]</sup> **7** [2.6230(8) Å]<sup>[4c]</sup> and  $\text{Pt}_2(\mu\text{-PPh}_2)_2(\text{PPh}_3)_2$  [2.604(1) Å],<sup>[10a]</sup> but shorter than that in platinum metal (2.774 Å).<sup>[11]</sup> These separations are in the expected range for  $\text{Pt}^{\text{I}}\text{–Pt}^{\text{I}}$  dinuclear derivatives.<sup>[12]</sup> Moreover, geometrical features also found in other  $[\text{M}_2(\mu\text{-PR}_2)_2(\text{L})(\text{L}')]$  complexes are the compressed Pt–P<sup>μ</sup>–Pt angles [av. 68.5(4)°], the large P<sup>μ</sup>–Pt–P<sup>μ</sup> angles (in

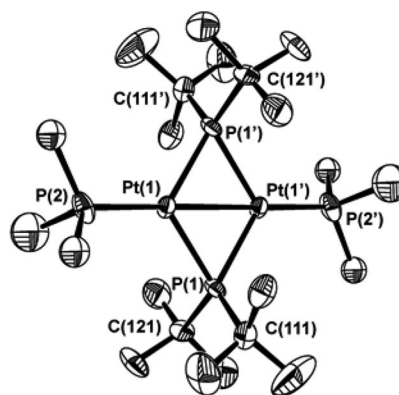


Figure 2. Perspective view of the molecular structure of **18**. Thermal ellipsoids are drawn at 30% probability. Primed atoms are obtained by the symmetry operation:  $-x + 1/2, -y + 1/2, -z + 1/2$ .

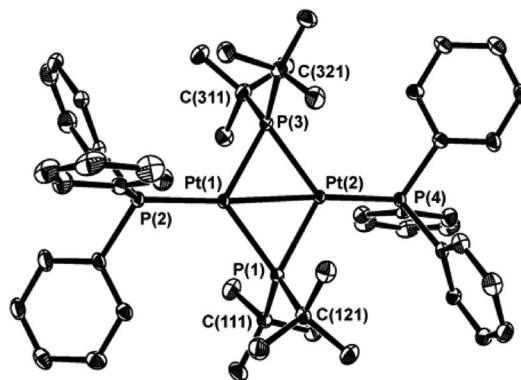


Figure 3. Perspective view of the molecular structure of **19**. Thermal ellipsoids are drawn at 30% probability.

Table 2. Selected bond lengths [Å] and angles [°] for **9**, **19**, **21**<sup>+</sup> and **18** (the numbering scheme used here is based on the least symmetric compound **19**; for the other compounds the corresponding distances are listed).

Compound	<b>9</b>	<b>18</b>	<b>19</b>	<b>21</b> <sup>+</sup>
Pt(1)–Pt(2)	2.5999(8)	2.6053(4)	2.6126(2)	2.6349(3)
Pt(1)–P(1)	2.322(2)	2.309(1)	2.322(1)	2.327(1)
Pt(2)–P(1)	2.318(2)		2.320(1)	2.3061(9)
Pt(1)–P(3)			2.315(1)	
Pt(2)–P(3)			2.318(1)	
Pt(1)–P(2)		2.214(2)	2.234(1)	2.2600(8)
Pt(1)–C(1)	1.86(1)			
Pt(2)–P(4)			2.234(1)	
Pt(1)–P(1)–Pt(2)	68.17(6)		68.51(3)	69.33(3)
Pt(1)–P(3)–Pt(2)		68.70(4)	68.65(4)	
P(1)–Pt(1)–P(2)		125.1(2)	127.92(5)	133.78(3)
P(1)–Pt(1)–C(1)	122.5(3)			
P(3)–Pt(1)–P(2)		123.6(2)	120.57(5)	115.57(4)
P(3)–Pt(1)–C(1)	125.7(3)			
P(1)–Pt(2)–P(4)			119.96(5)	
P(3)–Pt(2)–P(4)			128.61(5)	
P(1)–Pt(1)–P(3)	111.83(6)	111.30(4)	111.42(5)	110.67(3)
P(1)–Pt(2)–P(3)			111.41(5)	
P(2)–Pt(1)–Pt(2)		178.1(1)	175.59(4)	171.28(2)
C(1)–Pt(1)–Pt(2)	178.2(3)			
P(4)–Pt(2)–Pt(1)		178.1(1)	175.39(3)	

the range 111.3–114.4°) and the value of the P<sup>μ</sup>–Pt–L angles (in the range 120.0–128.6°). As usually found in bis(phosphido)-bridged derivatives of the group 10 metals, the Pt–P<sup>μ</sup> distances [2.309(2)–2.322(1) Å] are longer than the Pt–P<sup>t</sup> separations [2.214(2)–2.234(1) Å]. The reaction of a CD<sub>2</sub>Cl<sub>2</sub> solution of **19** with an equimolar amount of CF<sub>3</sub>SO<sub>3</sub>H results in the instantaneous and quantitative formation of the stable diplatinum(II) hydride [Pt<sub>2</sub>(μ-PtBu<sub>2</sub>)<sub>2</sub>(H)(PPh<sub>3</sub>)<sub>2</sub>]-CF<sub>3</sub>SO<sub>3</sub> (**21**). Analogously, asymmetrically substituted **12** is protonated rapidly to give [(*t*Bu<sub>2</sub>HP)Pt(μ-PtBu<sub>2</sub>)<sub>2</sub>Pt(H)(PPh<sub>3</sub>)]CF<sub>3</sub>SO<sub>3</sub> (**22a**). However, this is then quantitatively converted (τ<sub>1/2</sub> ca. 24 h) into its more stable isomer [(Ph<sub>3</sub>P)Pt(μ-PtBu<sub>2</sub>)<sub>2</sub>Pt(H)(PtBu<sub>2</sub>H)]CF<sub>3</sub>SO<sub>3</sub> (**22b**), the proton is attached to the platinum centre bonded to the more basic alkyl phosphane. A similar isomerisation was observed previously when **4** was protonated to give [(*t*Bu<sub>2</sub>HP)Pt(μ-PtBu<sub>2</sub>)<sub>2</sub>Pt(H)(CO)]CF<sub>3</sub>SO<sub>3</sub> (**6a**) and [(OC)Pt(μ-PtBu<sub>2</sub>)<sub>2</sub>Pt(H)(PtBu<sub>2</sub>H)]CF<sub>3</sub>SO<sub>3</sub> (**6b**).<sup>[4c]</sup>

The structures of complexes **21** and **22a,b** were inferred by analysing their <sup>1</sup>H, <sup>31</sup>P{<sup>1</sup>H} and <sup>195</sup>Pt{<sup>1</sup>H} NMR spectra (Table 3).

These are very similar to those discussed in detail for [Pt<sub>2</sub>(μ-PtBu<sub>2</sub>)<sub>2</sub>(H)(PtBu<sub>2</sub>H)]CF<sub>3</sub>SO<sub>3</sub> (**5**)<sup>[4b]</sup> and their analysis will not be duplicated here. Single crystals of **21** were obtained by slow evaporation of a CD<sub>2</sub>Cl<sub>2</sub>/toluene solution. The small values of <sup>2</sup>J(H<sup>1</sup>, P<sup>3</sup>) (<25 Hz) confirm that **21** and **22a,b** are true hydrides, that is, that the added proton H<sup>1</sup> is attached only to a metal centre with negligible interaction with the adjacent P<sup>3</sup>.<sup>[4b]</sup>

An ORTEP view of cation **21**<sup>+</sup> is shown in Figure 4, and relevant bond lengths and angles are reported in Table 2. As already found for cations **2**<sup>+</sup><sup>[3b,3c]</sup> and **5**<sup>+</sup>,<sup>[4a]</sup> the dinu-

Table 3. Selected NMR parameters for complexes **5**, **6a,b**, **21** and **22a,b**.

	L <sup>2</sup>	L <sup>4</sup>				
PPh <sub>3</sub>	PPh <sub>3</sub>	PPh <sub>3</sub>	<b>21</b>			
<i>Pr</i> Bu <sub>2</sub> H	PPh <sub>3</sub>	PPh <sub>3</sub>	<b>22a</b>			
PPh <sub>3</sub>	<i>Pr</i> Bu <sub>2</sub> H	PPh <sub>3</sub>	<b>22b</b>			
<i>Pr</i> Bu <sub>2</sub> H	CO	CO	<b>6a</b>			
CO	<i>Pr</i> Bu <sub>2</sub> H	<i>Pr</i> Bu <sub>2</sub> H	<b>6b</b>			
<i>Pr</i> Bu <sub>2</sub> H	<i>Pr</i> Bu <sub>2</sub> H	<i>Pr</i> Bu <sub>2</sub> H	<b>5</b>			

	<b>21</b>	<b>22a</b>	<b>22b</b>	<b>6a</b>	<b>6b</b>	<b>5</b>
δ(P <sup>3</sup> )	322	329	332	342.5	333.8	329.5
δ(P <sup>1</sup> )	351	361	339	393.5	369	348.0
δ(P <sup>4</sup> )	13.8	13.1	39.7	–	30.5	30.3
δ(P <sup>2</sup> )	42.3	65.9	42.5	62.1	–	57.5
δ(Pt <sup>1</sup> )	–5430	–5020	[a]	–5486	–5299	–5586
δ(Pt <sup>2</sup> )	–6055	–5586	[a]	–5936	–6163	–6268
δ(H <sup>1</sup> )	–2.5	–2.7	–3.5	–1.5	–2.6	–3.4
<sup>2</sup> J(P <sup>1</sup> , P <sup>3</sup> )	214	211	213	228	153	212
<sup>2</sup> J(P <sup>3</sup> , P <sup>4</sup> )	148	134	116	–	116	132
<sup>2</sup> J(P <sup>2</sup> , P <sup>3</sup> )	67	66	66	42	–	63
<sup>2</sup> J(P <sup>1</sup> , P <sup>4</sup> )	9	6	10	–	8	10
<sup>2</sup> J(P <sup>1</sup> , P <sup>2</sup> )	32	21	31	31	–	21
<sup>3</sup> J(P <sup>2</sup> , P <sup>4</sup> )	44	42	39	–	–	37
<sup>1</sup> J(Pt <sup>1</sup> , P <sup>3</sup> )	2756	2890	2722	2472	2855	2888
<sup>1</sup> J(Pt <sup>1</sup> , P <sup>1</sup> )	2327	2161	2472	2595	2202	2090
<sup>1</sup> J(Pt <sup>1</sup> , P <sup>2</sup> )	5116	4696	5160	4672	–	4762
<sup>1</sup> J(Pt <sup>2</sup> , P <sup>3</sup> )	796	737	1023	1273	833	934
<sup>1</sup> J(Pt <sup>2</sup> , P <sup>1</sup> )	1933	1746	1673	961	1484	1643
<sup>1</sup> J(Pt <sup>2</sup> , P <sup>4</sup> )	3651	3636	3025	–	2918	3034
<sup>1</sup> J(H <sup>1</sup> , Pt <sup>2</sup> )	602	604	610	679	683	690
<sup>2</sup> J(H <sup>1</sup> , P <sup>1</sup> )	91	101	98	80	99	109
<sup>2</sup> J(H <sup>1</sup> , P <sup>3</sup> )	≤23	≤22	≤24	10	14	14
<sup>2</sup> J(H <sup>1</sup> , P <sup>4</sup> )	≤23	≤22	≤24	–	25.5	28.5
<sup>1</sup> J(Pt <sup>1</sup> , Pt <sup>2</sup> )	300	250	[a]	617	390	340

[a] <sup>195</sup>Pt NMR spectroscopic data not available.

clear cation lies on a crystallographic inversion centre, thus only half of cation **21**<sup>+</sup> is independent. As a consequence of the imposed crystallographic symmetry, higher than the molecular one, the cation has identical coordination spheres around the two Pt centres due to an averaged disordered situation obtained by superimposing two different molecules across the centre of symmetry, in apparent contrast with the solution NMR spectroscopic data. It proved impossible to locate the Pt-bonded hydride, but its presence, unequivocally proved by NMR spectroscopic data, causes a significant distortion of the bond angles around the metal centres [P(1)–Pt(1)–P(2) 133.78(3)°, P(2)–Pt(1)–P(1') 115.57(3)°; see Figure 4]. The values of corresponding angles in precursor **19** are 120.57(5) and 127.92(5)°, respectively. The Pt–Pt distance [2.6349(3) Å] suggests that the Pt–Pt bond is retained, in accord with the calculated data in related cations **5**<sup>+</sup>–**6a,b**<sup>+</sup>,<sup>[4a,4c]</sup> despite the Pt<sup>II</sup> oxidation state of the two metal centres. Other parameters such as Pt–P<sup>μ</sup> [2.306(1) and 2.327(1) Å], Pt–P<sup>t</sup> 2.2600(8) Å and Pt(1)–P(1)–Pt(1') [69.33(3)°] are comparable to those observed in the parent derivatives. Finally, the asymmetry of the Pt–P<sup>μ</sup> bonds is less pronounced than in the agostic palladium cation **2**<sup>+</sup> [Pd–P<sup>μ</sup> 2.392(1) and 2.327(4) Å], in further accord with the different M...H interaction.

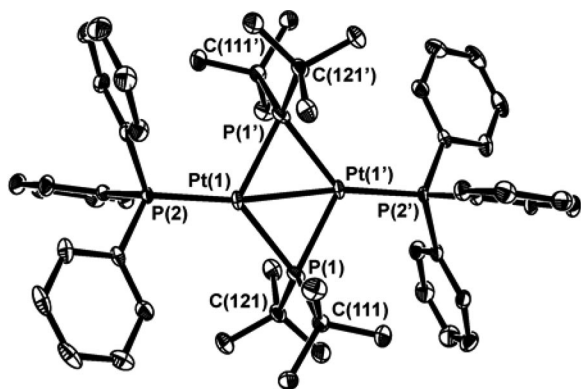


Figure 4. Perspective view of the molecular structure of cation **21**<sup>+</sup>. Thermal ellipsoids are drawn at 30% probability. Primed atoms are obtained by the symmetry operation:  $-x, -y, -z$ .

Contrary to **12** and **19**, complex **9** is protonated at phosphorus; the CD<sub>2</sub>Cl<sub>2</sub> solution obtained by treating **9** with an equimolar amount of CF<sub>3</sub>SO<sub>3</sub>H at  $-60^{\circ}\text{C}$  contains unique product **23** (Scheme 2), which contains one bridging phosphide [ $\delta(\text{P}^1) = 266.2$  ppm, d] and one terminally bonded secondary phosphane [ $\delta(\text{P}^2) = 51.4$  ppm, d;  $\delta(\text{H}^2) = 5.71$  ppm,  $^1J(\text{H}^2, \text{P}^2) = 388$  Hz,  $^2J(\text{H}^2, \text{Pt}^1) = 29$  Hz] in mutual *trans* position [ $^2J(\text{P}, \text{P}) = 200$  Hz]. The very large values of  $^1J(\text{H}^2, \text{P}^2)$  and  $^2J(\text{P}, \text{P})$  and the small value of  $^2J(\text{P}^2, \text{Pt}^2)$  (34 Hz) certify the absence of a  $\text{P}^2\text{--H--Pt}^2$  agostic interaction; moreover, the unusually large coupling between the bridging phosphorus nucleus and  $\text{Pt}^2$  (3971 Hz), obtained by  $^{31}\text{P}\{^1\text{H}\}$  and  $^{195}\text{Pt}\{^1\text{H}\}$  NMR spectra, implies a low coordination number for  $\text{Pt}^2$ .<sup>[4c]</sup> We therefore suggest that **23** has the structure shown in Scheme 2, with an unsaturated metal centre; similar structural features were assigned to  $[\text{Pd}_2(\mu\text{-PrBu}_2)(\text{PPh}_3)_3]\text{BF}_4$ <sup>[3d]</sup> in the related chemistry of palladium. Due to its unsaturation, complex **23** decomposes rapidly on warming to  $20^{\circ}\text{C}$  to give a complex mixture of unidentified products; however, it can be intercepted by operating under a carbon monoxide atmosphere. Under these conditions, the stable tricarbonyl derivative  $[\text{Pt}_2(\mu\text{-PrBu}_2)(\text{PrBu}_2\text{H})(\text{CO})_3]\text{CF}_3\text{SO}_3$  (see Experimental Section for NMR parameters) is quantitatively formed as a mixture of two isomers **24a,b** (Scheme 2). As compared to the related monophosphido-bridged derivative  $[\text{Pt}_2(\mu\text{-PrBu}_2)$

$(\text{PrBu}_2\text{H})_2(\text{CO})_2]\text{CF}_3\text{SO}_3$ ,<sup>[4d]</sup> for the presence of one less phosphane and one more carbonyl ligand, complex **24** is less sterically hindered and has less  $\pi$ -basic metals; therefore, it is more inclined to undergo carbonyl substitution reactions. For these reasons, both unsaturated derivative **23**, which can profitably be employed at low temperatures, and more stable **24** may be predicted to be useful starting materials for future reactivity studies.

## Conclusions

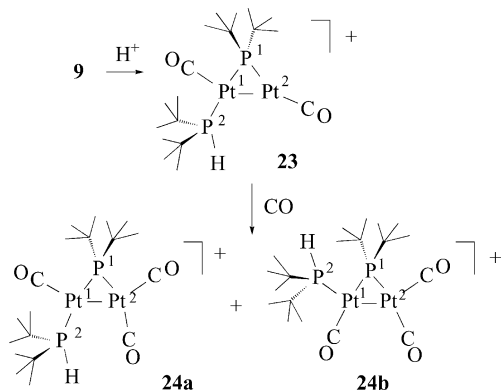
In this work we describe high-yielding synthetic procedures for the preparation of a series of bis(phosphido)-bridged derivatives with a common  $\text{Pt}_2(\mu\text{-PrBu}_2)_2$  core and a variable terminal ligand ( $\text{L}, \text{L}' = \text{CO}$ , secondary alkyl-, tertiary alkyl- or arylphosphanes) bonded to each platinum centre. The nature of  $\text{L}, \text{L}'$  influences considerably the path of the protonation of these complexes. When at least one of the terminal ligands  $\text{L}$  is a phosphane, the protonation occurs selectively at the metal centre.

If  $\text{L} \neq \text{L}'$ , the proton is attached first to the less-basic but less-hindered metal centre, but the kinetic  $\text{Pt}_2^{\text{II}}$  hydride isomerises slowly and quantitatively into its thermodynamic isomer, where the proton is attached to the metal bearing the better  $\sigma$  donor. As previously reported,<sup>[4c]</sup> monocarbonyl **4** behaves similarly, but, when the basicity of the metal centre is further reduced by introducing a second strong  $\pi$ -acceptor ligand, as in dicarbonyl **9**, a phosphorus atom of one of the bridges becomes the strongest basic centre of the molecule, and the reaction yields a monophosphido-bridged  $\text{Pt}_2^{\text{I}}$  derivative.

## Experimental Section

**General Data:** The reactions were carried out under a nitrogen atmosphere by using standard Schlenk techniques.  $[\text{Pt}_2(\mu\text{-PrBu}_2)_2(\text{PrBu}_2\text{H})(\text{CO})]$  (**4**) was prepared as described previously.<sup>[4b]</sup> Solvents were dried by conventional methods and distilled under nitrogen prior to use. IR spectra (nujol mulls, KBr) were recorded with a Perkin–Elmer FTIR 1725X spectrophotometer. NMR spectra were recorded with a Varian Gemini 200 BB instrument (199.98 MHz for  $^1\text{H}$ , 80.95 MHz for  $^{31}\text{P}$ , 42.76 MHz for  $^{195}\text{Pt}$ ); chemical shifts are referenced to the residual resonances of the deuterated solvent ( $^1\text{H}$ ,  $^{13}\text{C}$ ), 85%  $\text{H}_3\text{PO}_4$  ( $^{31}\text{P}$ ) and  $\text{H}_2\text{PtCl}_6$  ( $^{195}\text{Pt}$ ).  $^{31}\text{P}$  and  $^{195}\text{Pt}$  NMR spectroscopic data given in Tables 2 and 3 are not duplicated here; in NMR spectra dm stands for double multiplet, vt for virtual triplet. Elemental analyses were performed with a Carlo Erba model 1106 instrument.

**$[\text{Pt}(\mu\text{-PrBu}_2)(\text{CO})]_2$  (**9**):** An orange toluene (15 mL) solution of **4** (350 mg, 0.409 mmol) was transferred into a stainless steel autoclave. This was then evacuated and filled with dry  $\text{O}_2$  (50 mL, 2.2 mmol) and pressurised with CO (80 atm). After stirring for 12 h at room temperature, the autoclave was depressurised and left under an atmosphere of CO (1 atm). The resulting orange solution was transferred into a Schlenk tube and the solvent was evaporated, and the residue was suspended in acetone (10 mL). The suspension was filtered, and the air-stable orange solid was washed with acetone and vacuum dried (241 mg, 80% yield). The  $^{31}\text{P}\{^1\text{H}\}$  NMR spectrum of the filtrate exhibited a strong singlet at  $\delta =$



Scheme 2.

61.0 ppm, assignable to  $t\text{Bu}_2\text{HP}=\text{O}$ . Complex **9** was also obtained by warming a toluene solution of **4** at 60 °C for 12 h under an atmosphere of CO (1 atm) containing a stoichiometric amount of dry  $\text{O}_2$ . In this case, the final solution also contained ( $^{31}\text{P}\{^1\text{H}\}$  NMR) minor (<10%) amounts of other unidentified products.  $\text{C}_{18}\text{H}_{36}\text{O}_2\text{P}_2\text{Pt}_2$  (736.66): calcd. C 29.35, H 4.93; found C 29.23, H 5.06. IR (Nujol):  $\tilde{\nu} = 1980$  ( $\nu_{\text{CO}}$ )  $\text{cm}^{-1}$ .

**Reaction of 9 with  $\text{H}_2$  or Water:** An orange toluene (3 mL) solution of **9** (30 mg, 0.041 mmol) was transferred into a stainless steel autoclave and pressurised with  $\text{H}_2$  (180 atm). After stirring for 24 h at room temperature, the autoclave was depressurised, and the solution was transferred into a Schlenk tube. A  $^{31}\text{P}\{^1\text{H}\}$  NMR spectrum showed the formation (ca. 65%) of the known  $[\text{Pt}_3(\mu\text{-PrBu}_2)_3\text{-(H)(CO)}_2]$  (**10**)<sup>[5]</sup> with minor amounts of unidentified products. The same complex was formed, albeit in lower yields, when water was deliberately added to toluene solutions of complex **9**, or when the solvent was not carefully dried.

**Preparation of  $[\text{Pt}_2(\mu\text{-PrBu}_2)_2(\text{PrBu}_2\text{H})(\text{PR}_3)]$  [**11**, R = Me; **12**, R = Ph; **13**, R = Cy; **14**, R =  $\text{C}_2\text{H}_5$ ]**

**11:**  $\text{PMe}_3$  (11.0  $\mu\text{L}$ , 0.11 mmol) was added to an orange solution of  $[\text{Pt}_2(\mu\text{-PrBu}_2)_2(\text{PrBu}_2\text{H})(\text{CO})]$  (**4**; 90 mg, 0.10 mmol) in toluene (3 mL), and a pale-yellow solid quickly started to precipitate out. After the addition of *n*-hexane (10 mL) the suspension was stirred and left overnight at –30 °C. Complex **11** was isolated as a solid by filtration, which was then washed with *n*-hexane and vacuum dried (81 mg, 90% yield).  $\text{C}_{27}\text{H}_{64}\text{P}_4\text{Pt}_2$  (902.86): calcd. C 35.92, H 7.14; found C 36.03, H 7.06.  $^1\text{H}$  NMR ( $\text{CD}_2\text{Cl}_2$ , 293 K):  $\delta = 6.34$  [dm,  $^1J(\text{H,P}) = 317$  Hz,  $^2J(\text{H,Pt}) = 34$  Hz, 1 H, *PH*], 1.85 [d,  $^3J(\text{H,P}) = 8.6$  Hz,  $^3J(\text{H,Pt}) = 37$  Hz, 9 H, *PCH*], 1.38 [d,  $^3J(\text{H,P}) = 14$  Hz, 18 H, *HPCCCH*], 1.27 (br. vt, 36 H,  $\mu\text{-PCCCH}_3$ ) ppm.

**12:** Prepared analogously to **11**. Yield: 92%.  $\text{C}_{42}\text{H}_{70}\text{P}_4\text{Pt}_2$  (1089.08): calcd. C 46.32, H 6.48; found C 46.51, H 6.29.  $^1\text{H}$  NMR ( $\text{CD}_2\text{Cl}_2$ , 293 K):  $\delta = 7.76$  (m, 6 H,  $\text{C}_6\text{H}_5$ ), 7.30 (m, 9 H,  $\text{C}_6\text{H}_5$ ), 6.41 [d,  $^1J(\text{H,P}) = 320$  Hz,  $^2J(\text{H,Pt}) = 37$  Hz, 1 H, *PH*], 1.39 [d,  $^3J(\text{H,P}) = 14$  Hz, 18 H, *HPCCCH*], 1.21 (m, 36 H,  $\mu\text{-PCCCH}_3$ ) ppm.

**13:** Prepared analogously to **11**. Yield: 45%.  $\text{C}_{42}\text{H}_{88}\text{P}_4\text{Pt}_2$  (1107.22): calcd. C 45.56, H 8.01; found C 45.29, H 8.36.  $^1\text{H}$  NMR ( $\text{CD}_2\text{Cl}_2$ , 293 K):  $\delta = 6.31$  [dm,  $^1J(\text{H,P}) = 317$  Hz, 1 H, *PH*], 1.94–1.24 (br. m, 33 H, Cy), 1.37 [d,  $^3J(\text{H,P}) = 14$  Hz, 18 H, *HPCCCH*], 1.28 (m, 36 H,  $\mu\text{-PCCCH}_3$ ) ppm.

**14:** Prepared analogously to **11**. Yield: 89%.  $\text{C}_{36}\text{H}_{78}\text{P}_4\text{Pt}_2$  (1025.08): calcd. C 42.18, H 7.67; found C 42.30, H 7.81.  $^1\text{H}$  NMR ( $\text{CD}_2\text{Cl}_2$ , 293 K):  $\delta = 6.30$  [dm,  $^1J(\text{H,P}) = 317$  Hz, 1 H, *PH*], 6.07 [dm,  $^1J(\text{H,P}) = 315$  Hz, 1 H, *PH*], 1.94–1.23 (br. m, 22 H, Cy), 1.37 [d,  $^3J(\text{H,P}) = 14$  Hz, 18 H, *HPCCCH*], 1.28 (br. vt, 36 H, *PCCCH*) ppm.

**Preparation of  $[\text{Pt}_2(\mu\text{-PrBu}_2)_2(\text{CO})(\text{PR}_3)]$  [**15**, R = Me; **16**, R = Ph; **17**, R = Cy]**

**15:**  $\text{PMe}_3$  (7.0  $\mu\text{L}$ , 0.068 mmol) was added to an orange toluene (3 mL) solution of **9** (50 mg, 0.068 mmol). The colour of the solution faded immediately and the  $^{31}\text{P}\{^1\text{H}\}$  NMR spectrum showed the quantitative formation of **15**. The solvent was evaporated, and the residue was suspended in *n*-hexane (10 mL); the suspension was then stirred and left overnight at –30 °C. Complex **15** was isolated as an orange solid by filtration, which was then washed with *n*-hexane and vacuum dried (52 mg, 95% yield).  $\text{C}_{20}\text{H}_{45}\text{OP}_3\text{Pt}_2$  (784.66): calcd. C 30.61, H 5.78; found C 29.98, H 6.592. IR ( $\text{CH}_2\text{Cl}_2$ ):  $\tilde{\nu} = 1953$  ( $\nu_{\text{CO}}$ )  $\text{cm}^{-1}$ .  $^1\text{H}$  NMR ( $\text{CD}_2\text{Cl}_2$ , 293 K):  $\delta = 1.91$  [d,  $^2J(\text{H,P}) = 9$  Hz,  $^3J(\text{H,Pt}) = 41$  Hz, 9 H, *PCH*], 1.30–1.18 (m, 36 H, *PCCCH*) ppm.

**16:** Prepared analogously to **15**. Yield: 91%.  $\text{C}_{35}\text{H}_{51}\text{OP}_3\text{Pt}_2$  (970.87): calcd. C 43.30, H 5.30; found C 43.24, H 5.06. IR ( $\text{CH}_2\text{Cl}_2$ ):  $\tilde{\nu} = 1959$  ( $\nu_{\text{CO}}$ )  $\text{cm}^{-1}$ .  $^1\text{H}$  NMR ( $\text{CD}_2\text{Cl}_2$ , 293 K):  $\delta = 7.74$  (m, 6 H,  $\text{C}_6\text{H}_5$ ), 7.37 (m, 9 H,  $\text{C}_6\text{H}_5$ ), 1.21 (m, 36 H, *PCCCH*) ppm.

**17:** Prepared analogously to **15**. Yield: 86%.  $\text{C}_{35}\text{H}_{69}\text{OP}_3\text{Pt}_2$  (989.02): calcd. C 42.50, H 7.03; found C 42.81, H 7.16. IR ( $\text{CH}_2\text{Cl}_2$ ):  $\tilde{\nu} = 1948$  ( $\nu_{\text{CO}}$ )  $\text{cm}^{-1}$ .  $^1\text{H}$  NMR ( $\text{CD}_2\text{Cl}_2$ , 293 K):  $\delta = 2.16$ –1.22 (br. m, 33 H,  $\text{C}_6\text{H}_5$ ), 1.31 (m, 36 H, *PCCCH*) ppm.

**Preparation of  $[\text{Pt}(\mu\text{-PrBu}_2)(\text{PR}_3)]_2$  [**18**, R = Me; **19**, R = Ph; **20**, R = Cy]**

**18:**  $\text{PMe}_3$  (14.3  $\mu\text{L}$ , 0.14 mmol) was added to toluene solution (2 mL) of **9** (50 mg, 0.068 mmol), and a pale-yellow solid quickly precipitated out. After the addition of *n*-hexane (10 mL), the suspension was stirred and left overnight at –30 °C. Complex **18** was isolated as a solid by filtration, which was then washed with *n*-hexane and vacuum dried (49 mg, 84% yield).  $\text{C}_{22}\text{H}_{54}\text{P}_4\text{Pt}_2$  (832.73): calcd. C 31.73, H 6.54; found C 32.21, H 6.71.  $^1\text{H}$  NMR ( $\text{CD}_2\text{Cl}_2$ , 293 K):  $\delta = 1.80$  [d,  $^2J(\text{H,P}) = 8$  Hz,  $^3J(\text{H,Pt}) = 39$  Hz, 18 H, *PCH*], 1.21 (m, 36 H, *PCCCH*) ppm.

**19:** Prepared analogously to **18**. Yield: 85%.  $\text{C}_{52}\text{H}_{66}\text{P}_4\text{Pt}_2$  (1205.16): calcd. C 51.82, H 5.52; found C 51.59, H 5.35.  $^1\text{H}$  NMR ( $\text{CD}_2\text{Cl}_2$ , 293 K):  $\delta = 7.76$  (m, 6 H,  $\text{C}_6\text{H}_5$ ), 7.31 (m, 9 H,  $\text{C}_6\text{H}_5$ ), 1.06 (br. vt, 36 H,  $\mu\text{-PCCCH}_3$ ) ppm.

**20:** Prepared analogously to **18**. Yield: 83%.  $\text{C}_{52}\text{H}_{102}\text{P}_4\text{Pt}_2$  (1241.14): calcd. C 50.32, H 8.28; found C 50.26, H 8.07.  $^1\text{H}$  NMR ( $\text{CD}_2\text{Cl}_2$ , 293 K):  $\delta = 2.16$ –1.18 (br. m, 66 H, Cy), 1.32 (m, 36 H,  $\mu\text{-PCCCH}_3$ ) ppm.

**Protonation of 19:**  $\text{CF}_3\text{SO}_3\text{H}$  (2.2  $\mu\text{L}$ , 0.025 mmol) was added to an NMR tube containing a  $\text{CD}_2\text{Cl}_2$  (0.3 mL) suspension of **19** (30 mg, 0.025 mmol). The solid dissolved quickly, and the spectra of the orange solution showed only the resonances assigned to  $[\text{Pt}_2(\mu\text{-PrBu}_2)_2(\text{H})(\text{PPh}_3)_2]\text{CF}_3\text{SO}_3$  (**21**).  $^1\text{H}$  NMR ( $\text{CD}_2\text{Cl}_2$ , 293 K):  $\delta = 7.63$  (m, 12 H,  $\text{C}_6\text{H}_5$ ), 7.47 (m, 18 H,  $\text{C}_6\text{H}_5$ ), 1.20 [d,  $^3J(\text{H,P}) = 16$  Hz, 18 H, *PCCCH*], 0.91 [d,  $^3J(\text{H,P}) = 15$  Hz, 18 H, *PCCCH*], –2.49 [dt,  $^2J(\text{H,P}) = 95$ , 23 Hz,  $^1J(\text{H,Pt}) = 602$  Hz, 1 H, *Pt-H*] ppm.

**Protonation of 12:**  $\text{CF}_3\text{SO}_3\text{H}$  (2.7  $\mu\text{L}$ , 0.031 mmol) was added to an NMR tube containing a  $\text{CD}_2\text{Cl}_2$  (0.3 mL) suspension of **12** (34 mg, 0.031 mmol). The solid dissolved quickly, and the spectra of the orange solution showed only the resonances assigned to  $[(t\text{Bu}_2\text{HP})\text{Pt}(\mu\text{-PrBu}_2)_2\text{Pt}(\text{H})(\text{PPh}_3)]\text{CF}_3\text{SO}_3$  (**22a**). This disappeared slowly to leave, after 2 d, only the resonances of its isomer  $[(\text{Ph}_3\text{P})\text{Pt}(\mu\text{-PrBu}_2)_2\text{Pt}(\text{H})(\text{PrBu}_2\text{H})]\text{CF}_3\text{SO}_3$  (**22b**). Data for **22a**:  $^1\text{H}$  NMR ( $\text{CD}_2\text{Cl}_2$ , 293 K):  $\delta = 7.70$  (m, 15 H,  $\text{C}_6\text{H}_5$ ), 5.99 [dm,  $^1J(\text{H,P}) = 348$  Hz, 1 H, *P-H*], 1.29 (m, 54 H, *PCCCH*), –2.67 [dt,  $^2J(\text{H,P}) = 100$ , 19 Hz,  $^1J(\text{H,Pt}) = 618$  Hz, 1 H, *Pt-H*] ppm. Data for **22b**:  $^1\text{H}$  NMR ( $\text{CD}_2\text{Cl}_2$ , 293 K):  $\delta = 7.69$  (m, 6 H,  $\text{C}_6\text{H}_5$ ), 7.47 (m, 9 H,  $\text{C}_6\text{H}_5$ ), 6.00 [dm,  $^1J(\text{H,P}) = 340$  Hz, 1 H, *P-H*], 1.26 (m, 54 H, *PCCCH*), –3.50 [dt,  $^2J(\text{H,P}) = 96$ , 20 Hz,  $^1J(\text{H,Pt}) = 671$  Hz, 1 H, *Pt-H*] ppm.

#### Protonation of 9

**Method A:** Under a  $\text{N}_2$  atmosphere,  $\text{CF}_3\text{SO}_3\text{H}$  (3.7  $\mu\text{L}$ ,  $d = 1.69$   $\text{g mL}^{-1}$ , 0.19 mmol) was added to an NMR tube containing a  $\text{CD}_2\text{Cl}_2$  (0.5 mL) solution of **9** (30 mg, 0.041 mmol) at 213 K. The solution quickly turned brown, and the NMR spectrum (213 K) showed only the resonances assigned to complex **23**.  $^{31}\text{P}\{^1\text{H}\}$  NMR:  $\delta = 266.7$  [d,  $^2J(\text{P,P}) = 200$  Hz,  $^1J(\text{P}^1, \text{Pt}^2) = 3971$  Hz,  $^1J(\text{P}^1, \text{Pt}^1) = 2807$  Hz,  $\text{P}^1$ ], 51.4 [d,  $^2J(\text{P,P}) = 200$  Hz,  $^1J(\text{P}^2, \text{Pt}^1) = 2803$  Hz,  $^2J(\text{P}^2, \text{Pt}^2) = 34$  Hz,  $\text{P}^2$ ] ppm; in the corresponding proton coupled spectrum the main lines of the latter signal appear as a dd

[ $^2J(\text{P,P}) = 200 \text{ Hz}$ ,  $^1J(\text{P,H}) = 388 \text{ Hz}$ ].  $^{195}\text{Pt}\{^1\text{H}\}$  NMR:  $\delta = -4604$  [dd,  $^1J(\text{P,Pt}) = 3971 \text{ Hz}$ ,  $^2J(\text{P,Pt}) = 34 \text{ Hz}$ ,  $^1J(\text{Pt,Pt}) = 2332 \text{ Hz}$ ,  $\text{Pt}^2$ ],  $-4940$  [t,  $^1J(\text{P,Pt}) = 2807 \text{ Hz}$ ,  $^1J(\text{Pt,Pt}) = 2332 \text{ Hz}$ ,  $\text{Pt}^1$ ] ppm.  $^1\text{H}$  NMR:  $\delta = 5.71$  [d,  $^1J(\text{H,P}^2) = 388 \text{ Hz}$ ,  $^2J(\text{H,Pt}^1) = 29 \text{ Hz}$ , 1 H, P–H], 1.35 [d,  $^3J(\text{H,P}) = 16 \text{ Hz}$ , 18 H, C–H], 1.23 [d,  $^3J(\text{H,P}) = 15 \text{ Hz}$ , 18 H, C–H] ppm. When the temperature was raised to 298 K, the above-mentioned signals disappeared leaving a complex set of resonances due to unidentified decomposition products.

**Method B:** Under a CO atmosphere,  $\text{CF}_3\text{SO}_3\text{H}$  (3.4  $\mu\text{L}$ , 0.037 mmol) was added to an NMR tube containing a  $\text{CD}_2\text{Cl}_2$  (0.5 mL) solution of **9** (27 mg, 0.037 mmol). The colour of the solution faded immediately, and the spectra of the yellow solution showed only the resonances of the 3:2 mixture of two isomers of  $[\text{Pt}_2(\mu\text{-PrBu}_2)(\text{PtBu}_2\text{H})(\text{CO})_3]\text{CF}_3\text{SO}_3$  (**24a,b**).  $^1\text{H}$  NMR (293 K):  $\delta = 5.98$  [d,  $^1J(\text{H,P}^2) = 357 \text{ Hz}$ ,  $^2J(\text{H,Pt}^1) = 71 \text{ Hz}$ ,  $^3J(\text{H,Pt}^2) = 48 \text{ Hz}$ , P–H, **24b**], 5.64 [dd,  $^1J(\text{H,P}^2) = 362 \text{ Hz}$ ,  $^3J(\text{H,Pt}^1) = 6 \text{ Hz}$ ,  $^2J(\text{H,Pt}^1) = 60 \text{ Hz}$ , P<sup>2</sup>–H, **24a**], 1.43 (m,  $\text{PCCCH}_3$ ) ppm.  $^{31}\text{P}\{^1\text{H}\}$  NMR:  $\delta = 33.7$  [d,  $^2J(\text{P,P}) = 11 \text{ Hz}$ ,  $^1J(\text{P}^2,\text{Pt}^1) = 2993 \text{ Hz}$ ,  $^2J(\text{P}^2,\text{Pt}^2) = 285 \text{ Hz}$ ,  $\text{P}^2$ , **24b**], 48.8 [d,  $^2J(\text{P,P}) = 191 \text{ Hz}$ ,  $^1J(\text{P}^2,\text{Pt}^1) = 2536 \text{ Hz}$ ,  $^2J(\text{P}^2,\text{Pt}^2) = -44 \text{ Hz}$ ,  $\text{P}^2$ , **24a**], 265.3 [d,  $^2J(\text{P,P}) = 11 \text{ Hz}$ ,  $^1J(\text{P}^1,\text{Pt}^1) = 2944 \text{ Hz}$ ,  $^1J(\text{P}^1,\text{Pt}^2) = 2640 \text{ Hz}$ ,  $\text{P}^1$ , **24b**], 279.7 [d,  $^2J(\text{P,P}) = 191 \text{ Hz}$ ,  $^1J(\text{P}^1,\text{Pt}^2) = 2781 \text{ Hz}$ ,  $^1J(\text{P}^1,\text{Pt}^1) = 2394 \text{ Hz}$ ,  $\text{P}^1$ , **24a**] ppm; in the corresponding proton coupled spectrum the main lines of the signals at 33.7 (br. d) and 48.8 (dd) ppm are further split by the large value of  $^1J(\text{P,H})$  ca. 360 Hz].  $^{195}\text{Pt}\{^1\text{H}\}$  NMR:  $\delta = -5372$  [dd,  $^1J(\text{P,Pt}) = 2944$ , 2993 Hz,  $^1J(\text{Pt,Pt}) = 1850 \text{ Hz}$ ,  $\text{Pt}^1$ , **24b**],  $-5249$  [dd,  $^1J(\text{P,Pt}) = 2635 \text{ Hz}$ ,  $^2J(\text{P,Pt}) = 282 \text{ Hz}$ ,  $^1J(\text{Pt,Pt}) = 1850 \text{ Hz}$ ,  $\text{Pt}^2$ , **24b**],  $-5150$  [dd,  $^1J(\text{P,Pt}) = 2781 \text{ Hz}$ ,  $^2J(\text{P,Pt}) = -44 \text{ Hz}$ ,  $^1J(\text{Pt,Pt}) = 2600 \text{ Hz}$ ,  $\text{Pt}^2$ , **24a**],  $-5148$  [dd,  $^1J(\text{P,Pt}) = 2394$ , 2536 Hz,  $^1J(\text{Pt,Pt}) = 2600 \text{ Hz}$ ,  $\text{Pt}^1$ , **24a**]. Identical NMR spectra were observed when CO was bubbled at 213 K into the solution of complex **23** obtained as described in method a.

**Crystallography:** A red orange crystal of  $[\text{Pt}(\mu\text{-PrBu}_2)(\text{CO})_2]$  (**9**) was mounted on a Bruker P4 diffractometer, at room temperature for unit cell and space group determination and for the data collection. Red crystals of  $[\text{Pt}(\mu\text{-PrBu}_2)(\text{PMe}_3)]_2$  (**18**),  $[\text{Pt}(\mu\text{-PrBu}_2)(\text{PPh}_3)]_2$  (**19**) and  $[\text{Pt}_2(\mu\text{-PrBu}_2)_2(\text{H})(\text{PPh}_3)_2]\text{CF}_3\text{SO}_3$  (**21**) were mounted on a Bruker SMART CCD diffractometer for unit cell and space group determinations. Crystals of **19** and **21** were cooled to 200 K by using a cold nitrogen stream for the data collection. Selected crystallographic data are listed in Table 4. Data were corrected for Lorentz and polarisation factors by using the data reduction software SAINT<sup>[13]</sup> and empirically for absorption by using the SADABS program.<sup>[14]</sup> The structures were solved by Patterson, direct<sup>[15]</sup> and Fourier methods and refined by full-matrix least-squares<sup>[15]</sup> {the function minimised being  $\Sigma[w(F_o^2 - 1/kF_c^2)^2]$ }. For all structures, no extinction correction was deemed necessary. The scattering factors used, corrected for the real and imaginary parts of the anomalous dispersion, were taken from the literature.<sup>[16]</sup> All calculations were carried out by using the PC version of the programs WINGX<sup>[17]</sup> SHELX-97<sup>[15]</sup> and ORTEP<sup>[18]</sup>.

**Structural Study of  $[\text{Pt}(\mu\text{-PrBu}_2)(\text{CO})_2]$  (**9**):** The space group was unambiguously determined from the systematic absences, whereas the cell constants were refined by least-squares at the end of the data collection. Data acquisition was carried out by using a  $\omega/2\theta$  scan mode and collecting a redundant set of data. Three standard reflections, every 97, were measured to check the crystal decay: no significant variation was observed. The refinement was carried out by full-matrix least-squares by using anisotropic displacement parameters for the non-hydrogen atoms and isotropic for the hydrogen atoms that were included in the refinement using a riding model.

**Structural Study of  $[\text{Pt}(\mu\text{-PrBu}_2)(\text{PMe}_3)]_2$  (**18**):** The space group was unambiguously determined from the systematic absences, whereas the cell constants were refined by least-squares at the end of the data

Table 4. Crystal and structure refinement parameters for compounds **9**, **18**, **19**-( $\text{C}_7\text{H}_8$ ) and **21**.

Compound	<b>9</b>	<b>18</b>	<b>19</b> -( $\text{C}_7\text{H}_8$ )	<b>21</b>
Formula	$\text{C}_{18}\text{H}_{36}\text{O}_2\text{P}_2\text{Pt}_2$	$\text{C}_{22}\text{H}_{54}\text{P}_4\text{Pt}_2$	$\text{C}_{59}\text{H}_{74}\text{P}_4\text{Pt}_2$	$\text{C}_{53}\text{H}_{67}\text{F}_3\text{O}_3\text{P}_4\text{Pt}_2\text{S}$
$M$ [ $\text{g mol}^{-1}$ ]	736.59	832.71	1297.32	1355.19
Data Collection $T$ [K]	293(2)	293(2)	200(2)	200(2)
Radiation (Mo- $K_\alpha$ ) $\lambda$ [ $\text{\AA}$ ]	0.71073	0.71073	0.71073	0.71073
Crystal system	Monoclinic	Tetragonal	Orthorhombic	Triclinic
Space group (no.)	$P2_1/c$ (14)	$P4_2/n$ (86)	$P2_12_12_1$ (19)	$P\bar{1}$ (2)
$a$ [ $\text{\AA}$ ]	8.297(1)	13.2585(5)	15.3662(2)	10.8038(2)
$b$ [ $\text{\AA}$ ]	13.257(2)	13.2585(5)	18.4927(3)	11.9729(1)
$c$ [ $\text{\AA}$ ]	11.601(2)	18.471(1)	19.3189(1)	12.1202(2)
$\alpha$ [ $^\circ$ ]	90.0	90.0	90.0	70.635(1)
$\beta$ [ $^\circ$ ]	106.96(1)	90.0	90.0	79.001(1)
$\gamma$ [ $^\circ$ ]	90.0	90.0	90.0	77.229(1)
$V$ [ $\text{\AA}^3$ ]	1220.5(3)	3247.0(2)	5489.71(1)	1430.69(4)
$Z$	2	4	4	1
$\rho_{\text{calcd.}}$ [ $\text{g cm}^{-3}$ ]	2.004	1.703	1.570	1.572
$\mu$ [ $\text{cm}^{-1}$ ]	11.587	8.811	5.244	5.080
$\theta$ range [ $^\circ$ ]	2.39–24.99	2.17–29.34	1.52–27.45	1.95–27.49
Data collected	2872	20159	57017	14584
Independent data	2152	2209	12497	6449
Observed reflections	1548	1697	11324	5950
$[ F_o ^2 > 2.0\sigma( F_o ^2)]$				
Parameters refined	109	99	586	329
$R_{\text{int}}^{\text{[a]}}$	0.0341	0.0740	0.0372	0.0275
$R_1$ (obs. reflections) <sup>[b]</sup>	0.0347	0.0255	0.0275	0.0253
$wR_2$ (obs. reflections) <sup>[b]</sup>	0.0591	0.0590	0.0598	0.0624
GOF <sup>[c]</sup>	1.006	1.055	1.040	1.090

[a]  $R_{\text{int}} = \Sigma[F_o^2 - \langle F_o^2 \rangle] / \Sigma F_o^2$ . [b]  $R_1 = \Sigma(|F_o - (1/k)F_c|) / \Sigma |F_o|$ ;  $wR_2 = [\Sigma w(F_o^2 - (1/k)F_c^2)^2 / \Sigma w(F_o^2)^2]^{1/2}$ . [c]  $\text{GOF} = [\Sigma w(F_o^2 - (1/k)F_c^2)^2 / (n_o - n_v)]^{1/2}$ .

collection. The data were collected by using  $\omega$  scans, in steps of  $0.3^\circ$ . For each of the collected frames, counting time was 30 s. The least-squares refinement was carried out by using anisotropic displacement parameters for the P and C atoms of the phosphido-bridged moiety. The remaining atoms were treated isotropically. The large values of the displacement parameters of some atoms suggest the presence of structural disorder. The latter can be due to the higher crystallographic symmetry imposed on a less symmetric molecule, thus leading to positional disorder. An attempt to improve the refined model, by treating all atoms anisotropically, did not yield any significant improvement of the fit; therefore, the model with less parameters was retained. The contribution of the H atoms, in their calculated positions [ $C-H$   $0.96(\text{\AA})$ ,  $B(H) = 1.5 \times B(C_{\text{bonded}})(\text{\AA}^2)$ ], was included in the refinement by using a riding model.

**Structural Study of  $[\text{Pt}(\mu\text{-PrBu}_2)(\text{PPh}_3)_2]_2$  (19):** The space group was determined from the systematic absences. Cell constants were refined by least-squares at the end of the data collection. The data were collected by using  $\omega$  scans, in steps of  $0.3^\circ$ . For each of the 1800 collected frames, counting time was 20 s. The Fourier difference maps revealed a clathrated toluene molecule that was included in the refinement. The least-squares refinement was carried out by using anisotropic displacement parameters for all non-hydrogen atoms, whereas the H atoms were included in the refinement as described above [ $C-H$   $0.96(\text{\AA})$ ,  $B(H) = aB(C_{\text{bonded}})(\text{\AA}^2)$ ,  $a = 1.4$  for  $\text{CH}_3$  groups and  $1.2$  for the other H atoms].

**Structural Study of  $[\text{Pt}_2(\mu\text{-PrBu}_2)_2(\text{H})(\text{PPh}_3)_2]\text{CF}_3\text{SO}_3$  (21):** The values of the cell parameters were refined at the end of the data collection. The data were collected by using  $\omega$  scans, in steps of  $0.3^\circ$ . For each of the 1800 collected frames, counting time was 20 s. The space group assignment was confirmed by the successful refinement. Due to the crystallographic symmetry the asymmetric unit is half of the dimer; therefore, the counterion site occupancy factor (SOF) has to be 0.5. Refinement of the SOFs for the  $\text{CF}_3\text{SO}_3^-$  atoms confirmed this assumption. Refining the structure in the noncentrosymmetric space group P1 (thus almost doubling the number of refined parameters) did not yield a better fit or molecular geometry. It proved impossible to locate the hydride ligand (see the discussion of the structure). As often the case, the triflate show large amplitude motions for the atoms as a consequence of disorder that proved impossible to model satisfactorily. The least-squares refinement and H atoms treatment was carried out as described above.

CCDC-656030 (for **9**), -684894 (for **9-210**), -656031 (for **18**), -656032 (for **19**) and -656033 (for **21**) contain the supplementary crystallographic data for this publication. These data can be obtained free of charge from the Cambridge Crystallographic Data Centre via [www.ccdc.cam.ac.uk/data\\_request/cif](http://www.ccdc.cam.ac.uk/data_request/cif).

## Acknowledgments

This work was supported by the Ministero dell'Istruzione, dell'Università e della Ricerca (MIUR), Programmi di Rilevante Interesse Nazionale, PRIN 2006-2007 and by the University of Pisa (Progetti di Ricerca 2006 – Scienze e tecnologie dei nano/microsistemi).

- [1] a) J. Giver Planas, F. Hampel, J. A. Gladysz, *Chem. Eur. J.* **2005**, *11*, 1402–1416; b) D. K. Wicht, S. N. Paisner, B. M. Lew, D. S. Glueck, G. P. A. Yap, L. M. Liable-Sands, A. Rheingold, C. M. Haar, S. P. Nolan, *Organometallics* **1998**, *17*, 652–660; c) B. D. Zwick, M. A. Dewey, D. A. Knight, W. E. Buhro, A. M.

- Arif, J. A. Gladysz, *Organometallics* **1992**, *11*, 2673–2685; d) D. Scott Bohle, G. R. Clark, C. E. F. Rickard, W. R. Roper, *J. Organomet. Chem.* **1990**, *393*, 243–285; e) W. Malish, R. Maisch, I. J. Colquhoun, W. McFarlane, *J. Organomet. Chem.* **1981**, *220*, C1–C6; f) V. Gallo, M. Latronico, P. Mastroilli, C. F. Nobile, G. Ciccarella, U. Englert, *Eur. J. Inorg. Chem.* **2006**, 2634–2641; g) E. J. Derrah, D. A. Pantazis, R. McDonald, L. Rosenberg, *Organometallics* **2007**, *26*, 1473–1482; h) G. L. Geoffroy, S. Rosenberg, P. M. Schulman, R. R. Whittle, *J. Am. Chem. Soc.* **1984**, *106*, 1519–1521.
- [2] a) C. Archambault, R. Bender, P. Braunstein, Y. Dusauroy, *J. Chem. Soc., Dalton Trans.* **2002**, 4084–4090; b) H.-C. Böttcher, M. Graf, K. Merzweiler, C. Wagner, *J. Organomet. Chem.* **2001**, *628*, 144–150; c) P. Braunstein, E. de Jesus, A. Dedieu, M. Lanfranchi, A. Tiripicchio, *Inorg. Chem.* **1992**, *31*, 399–410; d) J. Powell, J. F. Sawyer, S. J. Smith, *J. Chem. Soc., Dalton Trans.* **1992**, 2793–2801; e) J. A. Cabeza, F. J. Lahoz, A. Martin, *Organometallics* **1992**, *11*, 2754–2756; f) R. Walther, H. Hartung, H.-C. Böttcher, U. Baumeister, U. Böhlend, J. Rheinold, J. Siler, J. Ladriere, H.-M. Schiebel, *Polyhedron* **1991**, *10*, 2423–2435; g) J. Powell, E. Fuchs, M. R. Gregg, J. Phillips, M. V. R. Stainer, *Organometallics* **1990**, *9*, 387–393; h) T. Adatia, M. McPartlin, M. J. Mays, M. J. Morris, P. R. Raithby, *J. Chem. Soc., Dalton Trans.* **1989**, 1555–1564; i) J. Powell, J. F. Sawyer, M. V. R. Stainer, *Inorg. Chem.* **1989**, *28*, 4461–4470; j) T. Blum, P. Braunstein, *Organometallics* **1989**, *8*, 2497–2503; k) B. Klingert, H. Werner, *J. Organomet. Chem.* **1987**, *333*, 119–128; l) L. Chen, D. J. Kountz, D. W. Meek, *Organometallics* **1985**, *4*, 598–601; m) H. Werner, W. Hofmann, R. Zolk, L. F. Dahl, J. Kocal, A. Kühn, *J. Organomet. Chem.* **1985**, *289*, 173–188.
- [3] a) P. Leoni, M. Sommovigo, M. Pasquali, P. Sabatino, D. Braga, *J. Organomet. Chem.* **1992**, *423*, 263–270; b) P. Leoni, M. Pasquali, M. Sommovigo, F. Laschi, P. Zanello, A. Albinati, F. Lianza, P. S. Pregosin, H. Rüegger, *Organometallics* **1993**, *12*, 1702–1713; c) P. Leoni, G. Pieri, M. Pasquali, *J. Chem. Soc., Dalton Trans.* **1998**, 657–662; d) P. Leoni, M. Pasquali, G. Pieri, A. Albinati, P. S. Pregosin, H. Rüegger, *Organometallics* **1995**, *14*, 3143–3145; e) P. Leoni, M. Pasquali, M. Sommovigo, A. Albinati, F. Lianza, P. S. Pregosin, H. Rüegger, *Organometallics* **1993**, *12*, 4503–4508; f) P. Leoni, E. Vichi, S. Lencioni, M. Pasquali, E. Chiarentin, A. Albinati, *Organometallics* **2000**, *19*, 3062–3068.
- [4] a) P. Leoni, M. Pasquali, A. Fortunelli, G. Germano, A. Albinati, *J. Am. Chem. Soc.* **1998**, *120*, 9564–9673; b) P. Leoni, G. Chiaradonna, M. Pasquali, F. Marchetti, *Inorg. Chem.* **1999**, *38*, 253–259; c) P. Leoni, M. Pasquali, V. Cittadini, A. Fortunelli, M. Selmi, *Inorg. Chem.* **1999**, *38*, 5257–5265; d) V. Cittadini, P. Leoni, L. Marchetti, M. Pasquali, A. Albinati, *Inorg. Chim. Acta* **2002**, *330*, 25; e) P. Leoni, F. Marchetti, L. Marchetti, V. Passarelli, *Chem. Commun.* **2004**, 2346–2347.
- [5] P. Leoni, S. Manetti, M. Pasquali, A. Albinati, *Inorg. Chem.* **1996**, *35*, 6045–6052.
- [6] M. P. Brown, R. J. Puddephatt, M. Rashidi, K. R. Seddon, *J. Chem. Soc., Dalton Trans.* **1978**, 516–522.
- [7] P. E. Garrou, *Chem. Rev.* **1981**, *81*, 229–266.
- [8] a)  $\text{Ni}_2[\mu\text{-P}(\text{SiMe}_3)_2](\text{PMe}_3)_2$ : B. Deppisch, H. Schafer, *Z. Anorg. Allg. Chem.* **1982**, *490*, 129–135; b)  $\text{Ni}_2(\mu\text{-PrBu}_2)_2(\text{PMe}_3)_2$ : R. A. Jones, A. L. Stuart, J. L. Atwood, W. E. Hunter, R. D. Rogers, *Organometallics* **1982**, *1*, 1721–1723; c)  $\text{Ni}_2(\mu\text{-PCy}_2)_2(\eta^2\text{-CH}_2=\text{CH}_2)_2$ : B. L. Barnett, C. Kruger, *Cryst. Struct. Commun.* **1973**, *2*, 85; d)  $\text{Ni}_2(\mu\text{-PCy}_2)_2(\text{PMeCy}_2)_2$ : C. E. Krilley, C. J. Woolley, M. K. Krepps, E. M. Popa, P. E. Fanwick, I. P. Rothwell, *Inorg. Chim. Acta* **2000**, *300*, 200–205.
- [9] a)  $\text{Pd}_2(\mu\text{-PrBu}_2)_2(\text{PMe}_3)_2$ : A. M. Arif, D. E. Heaton, R. A. Jones, C. M. Nunn, *Inorg. Chem.* **1987**, *26*, 4228–4231; b)  $\text{Pd}_2(\mu\text{-PCy}_2)_2[\text{P}(\text{OPh})\text{Cy}_2]_2$ : M. Sommovigo, M. Pasquali, P. Leoni, U. Englert, *Inorg. Chem.* **1994**, *33*, 2686–2688; c)  $\text{Pd}_2(\mu\text{-PrBu}_2)_2(\text{PEt}_3)_2$ : U. Englert, E. Matern, J. Olkowska-Oetzel, J. Piekies, *Acta Crystallogr., Sect. E: Struct. Rep. Online* **2003**, *59*, m376–m377.

- [10] a)  $\text{Pt}_2(\mu\text{-PPh}_2)_2(\text{PPh}_3)_2$ : N. J. Taylor, P. C. Chieh, A. J. Carty, *J. Chem. Soc., Chem. Commun.* **1975**, 448–449; b)  $\text{Pt}_2(\mu\text{-PCy}_2)_2(\text{PCy}_2\text{OR})_2$ : V. Gallo, M. Latronico, P. Mastrorilli, C. F. Nobile, G. P. Suranna, G. Ciccarella, U. Englert, *Eur. J. Inorg. Chem.* **2005**, 4607–4616.
- [11] Calculated from data reported on card 4–802 of the Powder Diffraction File of JCPDS-ICDD, International Center of Diffraction Data, **1992**, 12 Campus Boulevard, Newton Square, PA 19073–3273.
- [12] a) J. R. Fisher, A. J. Mills, S. Sumner, M. P. Brown, M. A. Thomson, R. J. Puddephatt, A. A. Frew, L. Manojlovic-Muir, K. W. Muir, *Organometallics* **1982**, *1*, 1421–1429; b) Y. Koie, S. Shinoda, Y. Saito, B. J. Fitzgerald, C. G. Pierpont, *Inorg. Chem.* **1980**, *19*, 770–773; c) R. Uson, J. Fornies, P. Espinet, C. Fortunato, M. Tomas, A. J. Welch, *J. Chem. Soc., Dalton Trans.* **1989**, 1583–1587; d) G. Minghetti, A. L. Bandini, G. Banditelli, F. Bonati, R. Szostak, C. E. Strouse, C. B. Knobler, H. D. Kaez, *Inorg. Chem.* **1983**, *22*, 2332–2338; e) R. Bender, P. Braunstein, A. Tiripicchio, M. Tiripicchio-Camellini, *J. Chem. Soc., Chem. Commun.* **1984**, 42–43; f) N. M. Boag, *Organometallics* **1988**, *7*, 1446–1449; g) V. Gallo, M. Latronico, P. Mastrorilli, C. F. Nobile, F. Polini, N. Re, U. Englert, *Inorg. Chem.* **2008**, *47*, 4785–4795.
- [13] BrukerAXS, *SAINT: Integration Software*, Bruker Analytical X-ray Systems, Madison, WI, **1995**.
- [14] G. M. Sheldrick, *SADABS: Program for Absorption Correction*, University of Göttingen, Göttingen, Germany, **1996**.
- [15] G. M. Sheldrick, *SHELX-97: Structure Solution and Refinement Package*, University of Göttingen, **1997**.
- [16] A. J. C. Wilson (Ed.), *International Tables for X-ray Crystallography*, Kluwer Academic, Dordrecht, The Netherlands, **1992**, vol. C.
- [17] L. J. Farrugia, *J. Appl. Crystallogr.* **1999**, *32*, 837–838.
- [18] L. J. Farrugia, *J. Appl. Crystallogr.* **1997**, *30*, 565.

Received: April 30, 2008

Published Online: August 12, 2008